[5]Hsu, C.-H., Hartwich, P.-M., and Liu, C. H.,"Incompressible Navier–Stokes Computations for a Rounded-Edged Double-Delta Wing," *Journal of Aircraft*, Vol. 25, No. 8, 1988, pp. 675, 676.

[6]Fujii, K., and Schiff, L. B., "Numerical Simulation of Vortical Flows over Strake-Delta Wing," *Journal of Aircraft*, Vol. 27, No. 9, 1989, pp. 1153–1162.

[7]Gordnier, R. E., and Visbal, M. R., "Unsteady Vortex Structure over a Delta Wing," *Journal of Aircraft*, Vol. 31, No. 2, 1994, pp. 243–248.

[8]Ishizaka, K., Ikohagi, T., and Daiguji, H., "A High-Resolution Finite Difference Scheme for Supersonic Wet-Stream Flows," *Transactions of the Japan Society of Mechanical Engineers, Series B*, Vol. 60, No. 579, 1994, pp. 3887–3892 (in Japanese).

[9]Frenkel, J., *Kinetic Theory of Liquids*, Dover, New York, 1955, Chap. 7.

[10]Yamamoto, S., and Daiguji, H., "Higher-Order-Accurate Upwind Schemes for Solving the Compressible Euler and Navier–Stokes Equations," *Computers and Fluids*, Vol. 22, No. 2/3, 1993, pp. 259–270.

[11]Yuan, X., Yamamoto, S., and Daiguji, H., "A Higher-Resolution Shock-Capturing Scheme for Simulating Unsteady Three-Dimensional Transonic Flows in Turbomachinery," AIAA Paper 94-3199, July 1994.

A. Plotkin
Associate Editor

Trailing Vortices from a Wing with a Notched Lift Distribution

W. R. Graham,* S.-W. Park,† and T. B. Nickels‡
University of Cambridge,
Cambridge, England CB2 1PZ, United Kingdom

Nomenclature

c	=	wing chord
c_l	=	section lift coefficient
R	=	chordwise radius of curvature
s	=	span of half-wing
U	=	towing speed
y, z	=	spanwise and normal coordinates
α_{local}	=	section incidence angle
Γ	=	section circulation

Introduction

INCREASING demands on airport capacity and the imminent arrival of the Airbus A380 super-Jumbo have refocused research and regulatory attention on the hazard associated with an aircraft's trailing vortices. Thus, from a manufacturer's viewpoint, configuration modifications that alleviate these vortices are potentially desirable.

In a recent paper,[1] Graham used two-dimensional vortex method calculations to show that significant reductions in the rolling moment induced on a following aircraft were predicted for notched wing lift distributions. Here a region of counter-rotating vorticity is shed between the flap outboard and wing tip vortices, which prevents their merger. This region is unlike the counter-rotating vortex typically generated by the aircraft's tail, in that it never rolls up into a distinct axisymmetric structure, instead becoming wrapped around the tip vortex. For a follower with wingspan 50% of that of the generator, the predicted reductions in rolling moment were around 20–25%.

One possible interpretation of these gains is that they fall short of the improvement required. This argument is based on results described in Rossow's recent review paper,[2] where a "vortex dissipater" mounted on a Convair 990 reduced the roll accelerations induced on a following Lear jet from 4.4 to 2.4 rad/s^2 without altering the pilot-perceived hazard. This, however, was because the lower acceleration still comfortably exceeded the Lear jet's roll authority, a feature that is clearly dependent on the size of both the generator and the follower. One could equally well envisage a situation where a 25% reduction in rolling moment brought it down to a level within the follower's roll authority. Thus, an alternative interpretation is that such a gain would alleviate the hazard associated with a 360-t landing weight aircraft to a level comparable with a 270-t B747-400. Additionally, the corresponding four-vortex system would be potentially susceptible to the accelerated instabilities reported by Crouch et al.[3]

The potential benefits of notched lift distributions were, therefore, deemed sufficient to seek experimental verification of the numerical predictions. This Note describes initial, proof-of-concept results from the experimental program.

Apparatus and Method

To follow the wake evolution as far as possible, the tests were carried out in a towing tank. The tank is 17.5 m long and 0.59 m wide and was filled to a depth of 0.6 m.

Two model half-wings, designed to exhibit conventional and notched high-lift distributions, were tested. (The use of half-wings, with root located at the water surface, increases the allowable model size and eliminates support interference.) Each has a (semi-) span of 300 mm and a mean chord of 100 mm, resulting in an effective aspect ratio of 6. Their cross sections have a cambered-plate geometry (to avoid the low-Reynolds-number problems associated with conventional airfoil sections), with thickness of 2 mm, radius of curvature of 210 mm, and nose radius of 1 mm. The leading edges are straight, and the required loading variations are achieved by varying the chord length. The conventional wing has a rectangular flap planform, with chord of 106 mm over the inner 183 mm of span and 90 mm over the remainder. The notched wing has constant chord sections of 105 and 102 mm over the inner 135 mm and outer 75 mm, with a smoothly varying notch of minimum chord 77 mm in between.

The wing planforms, along with lift distributions evaluated using lifting line theory,[4] are shown in Fig. 1. Section properties for this calculation, estimated on the basis of Schmitz's experimental results for the Göttingen 417a cambered plate aerofoil,[5] were

$$c_l = 2.75\pi\alpha_{\text{local}} + 1.16c/R \tag{1}$$

The notched distribution closely matches the optimum identified in Sec. III of Ref. 1. The conventional loading has the same overall lift coefficient, 0.43, and almost identical root circulation (which determines the overall circulation shed into the wake). The induced drag factors (relative to elliptic loading) are 1.12 and 1.04, respectively.

The tests were conducted at a towing speed of 0.534 m/s, corresponding to a (mean-chord-based) Reynolds number of 5.34×10^4. The wings were impulsively set in motion from 3.7 m down the tank, and the associated wake velocities were measured using digital particle image velocimetry (DPIV) at a crossflow plane 2.1 m farther downstream. The PIV system is a commercial model produced by Dantec and consists of a New Wave Research Gemini PIV 15 Nd: YAG laser, an MASD, Inc., Megaplus Model ES 4.0 digital camera, and a data acquisition/control unit linked to a personal computer. The seeding particles used have a diameter of 100 μm and relative density 1.0 ± 0.02. After seeding, the PIV system was used to check that the resulting fluid motions had decayed before a run was started.

Velocity fields were derived from the raw data using Dantec's proprietary cross-correlation software on pairs of images separated

Received 2 October 2002; revision received 2 April 2003; accepted for publication 7 April 2003.

*Senior Lecturer, Department of Engineering, Fluid Mechanics Group, Trumpington Street; wrg@eng.cam.ac.uk.

†Research Student, Department of Engineering, Fluid Mechanics Group, Trumpington Street.

‡Lecturer, Department of Engineering, Fluid Mechanics Group, Trumpington Street.

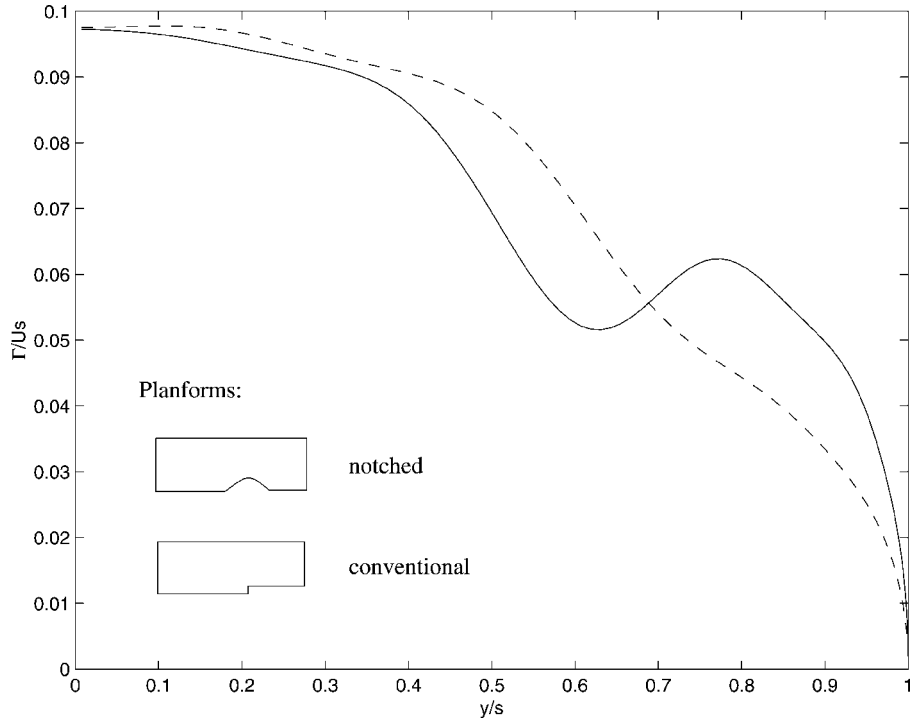

Fig. 1 Lift distributions for the conventional and notched wings: ——, notched and - - - -, conventional.

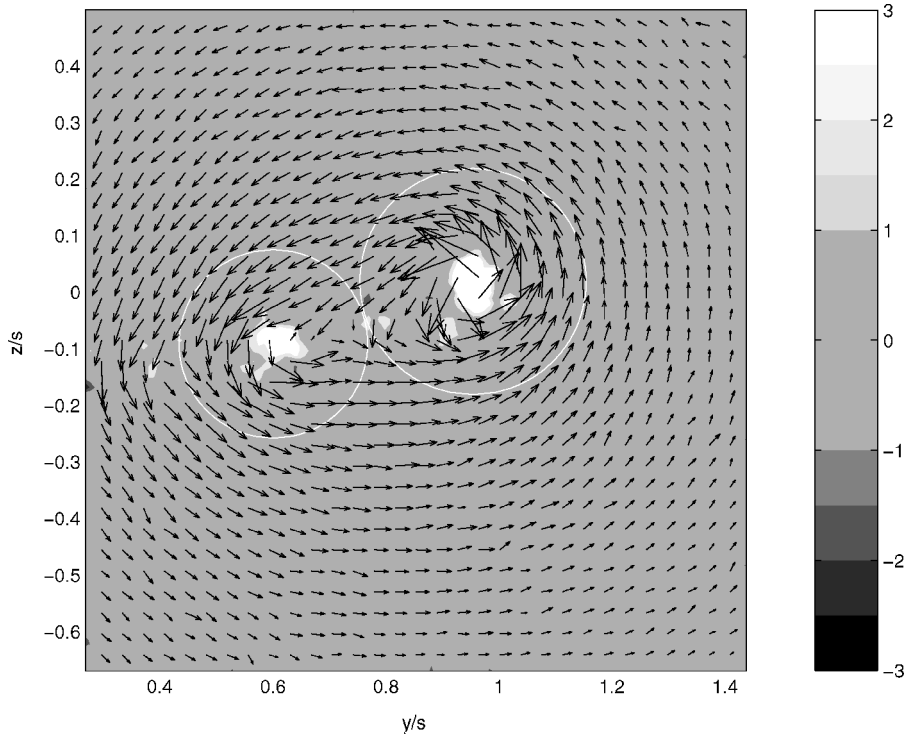

Fig. 2 Velocity vectors and corresponding contours of dimensionless vorticity, $\omega s/U$, 0.67 s after the passage of the conventional wing; circles indicate the integration areas for the flap and tip vortex circulation estimates of Table 1.

by 1 ms, each split into windows of size 64×64 pixels (10.52×10.52 mm). Range validation and comparison with adjacent vectors were used to identify outliers, which were subsequently replaced either by the next most likely value (if possible), or by the surrounding average. Typically, around 2% of the raw velocity data required this treatment. Four field realizations were then averaged to reduce estimation errors further. More extensive averaging was deemed unnecessary because preliminary flow visualization had shown no significant unsteadiness or instability.

Results and Discussion

Figures 2 and 3 show the measured velocity vectors (subsampled for clarity) and derived vorticity field for the conventional and notched wings 0.67 s after their passage through the measurement plane, which is thus 1.2 semispans downstream of the trailing edge.

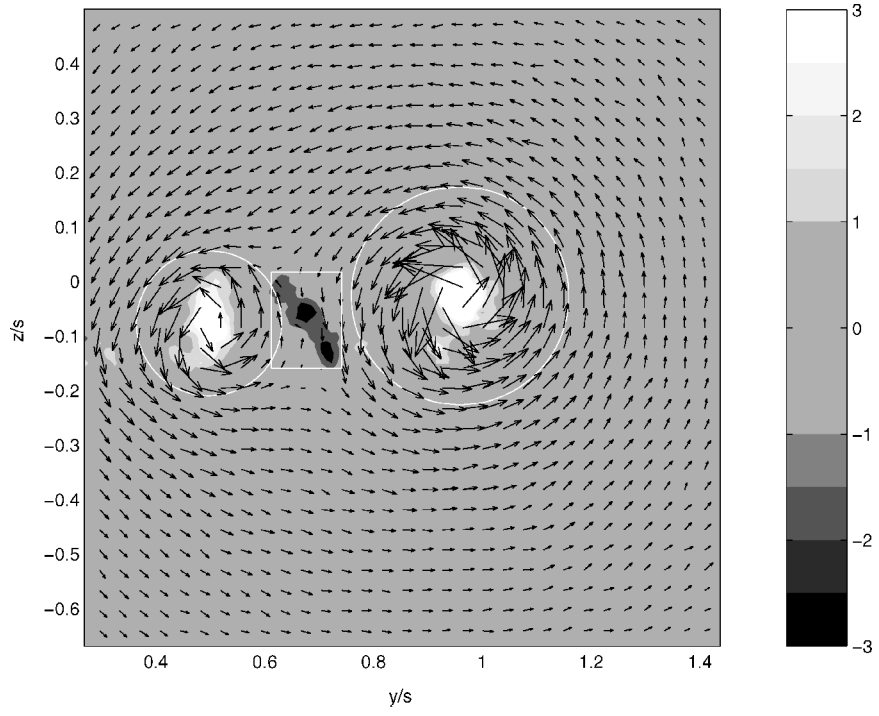

Fig. 3 Velocity vectors and corresponding contours of dimensionless vorticity, $\omega s/U$, 0.67 s after the passage of the notched wing. Note the region of negative vorticity, with shading darker than the freestream; circles and rectangle indicate the integration areas for the flap vortex, tip vortex, and negative region circulation estimates of Table 1.

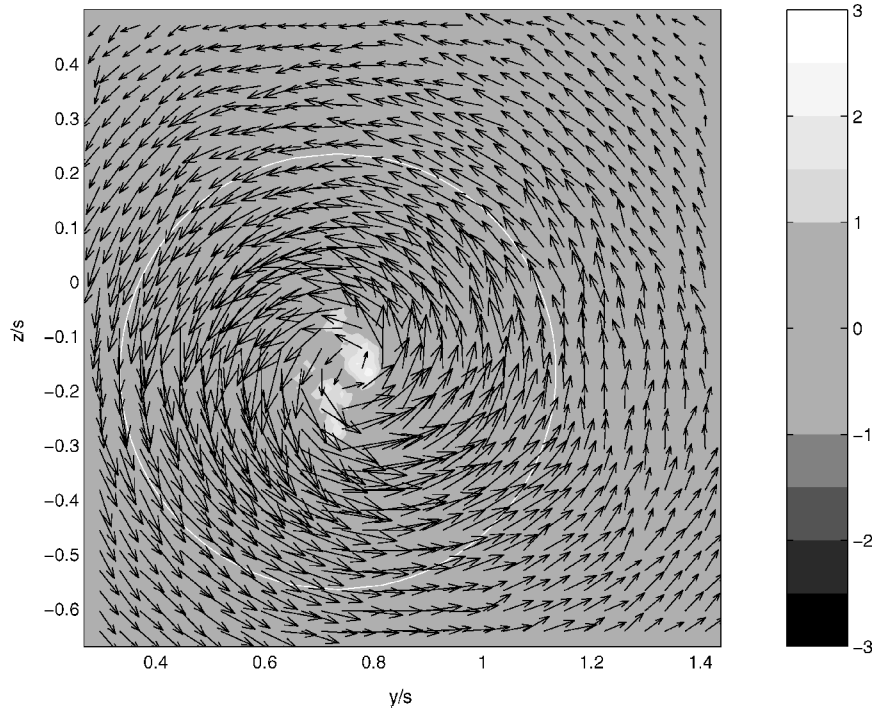

Fig. 4 Velocity vectors and corresponding contours of dimensionless vorticity, $\omega s/U$, 22.33 s after the passage of the conventional wing; circle indicates the integration area for the merged vortex circulation estimate of Table 1.

The corresponding plots after 22.33 s (39.7 semispans) are presented in Figs. 4 and 5.

It is immediately clear that both wings initially shed distinct flap and tip vortices, which subsequently merge in the case of the conventional wing, but remain distinct for the notched model. Closer inspection of the vorticity field immediately behind the latter (Fig. 3) also reveals a sheet of negative vorticity connecting the vortices. In contrast, no such region exists for the conventional wing (Fig. 2). Farther downstream (Figs. 4 and 5) neither vorticity field exhibits significant negative features.

Quantitative measures of the vorticity fields are given in Table 1. As expected, the initial overall circulation is almost identical for the two wings but is 10–13% higher than the predicted root circulation ($\Gamma/Us = 0.097$). At the later time, a slight decrease is observed for the conventional wing, possibly due to the limited measurement region. Initial flap vortex circulations are consistent with the predicted lift

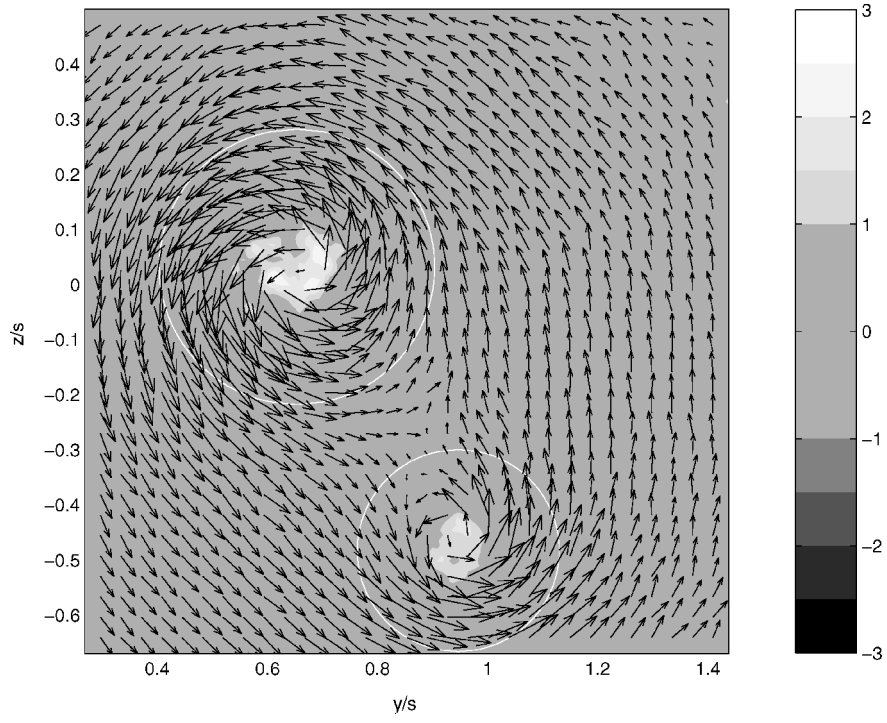

Fig. 5 Velocity vectors and corresponding contours of dimensionless vorticity, $\omega s/U$, 22.33 s after the passage of the notched wing; circles indicate the integration areas for the flap and tip vortex circulation estimates of Table 1.

Table 1 Quantitative measures of the vorticity fields[a]

Measure	Time, s	Conventional	Notched
Total circulation	0.67	0.107	0.110
	22.33	0.099	0.108
Flap vortex circulation	0.67	0.038	0.045
	22.33	N/A	0.034
Tip/merged vortex circulation	0.67	0.059	0.074
	22.33	0.093	0.067
Negative region circulation	0.67	N/A	−0.016
Spanwise centroid location	0.67	0.771	0.772
	22.33	0.769	0.760
Normal centroid location	0.67	−0.040	−0.063
	22.33	−0.178	−0.150

[a]Circulations are nondimensionalized on Us and centroid locations on s.

distributions, but tip vortex circulations are somewhat higher than expected in each case, as is the magnitude of the negative region circulation. Later, the merged vortex from the conventional wing has circulation close to the sum of the flap and tip contributions, whereas the separate vortices from the notched wing have circulations decreased from their initial values by roughly equal amounts. The sum of these decreases matches the negative region circulation. Finally, all fields have essentially identical spanwise vorticity centroid locations, slightly outboard of the predictions from the lift distributions ($0.74s$).

The experiment thus confirms the central prediction of Ref. 1, that the flap and tip vortices shed by a wing with a notched lift distribution remain distinct instead of merging. It also supports, to some extent, the hypothesis that this is due to an interposed, counter-rotating vortex sheet. However, although such a sheet is visible initially, it cannot later be seen wrapped around the tip vortex (as predicted by the simulations). The most probable explanation is that it has been annihilated, via diffusive effects, by positive vorticity; hence the reductions in tip and flap vortex circulations. For this to have happened, though, it must have been wrapped around both tip and flap vortices, rather than tip alone.

At this stage, the question of the possible benefits of this phenomenon remains open. However, it should be reiterated that the long-term separation of flap and tip vortices has the potential to reduce follower rolling moments appreciably and/or to allow the development of rapidly growing instabilities. The concept thus appears worthy of more detailed investigation.

Conclusions

In this Note, a proof-of-concept tow-tank experiment on a novel, notched form of wing lift distribution has been described. The results confirm the fundamental conclusion of earlier numerical simulations,[1] namely, that the flap and tip vortices shed by a wing with the novel distribution remain distinct and unmerged, unlike those associated with conventional high-lift distributions. This feature will lead to a reduced rolling moment on a follower aircraft encountering the wake and may also facilitate the development of rapidly growing instability modes. It is thus a promising avenue for wake hazard reduction and worthy of further work. This will consist of hazard reduction quantification and elucidation of the underlying mechanisms in more detail.

Acknowledgments

The work described here was carried out within the "C-Wake" project, funded by the European Community (Project GRD1-1999-10332). The Scientific Officer responsible for C-Wake was Dietrich Knoerzer, and it was coordinated by Klaus Huenecke of Airbus Deutschland.

References

[1]Graham, W. R., "Optimising Wing Lift Distribution to Minimize Wake Vortex Hazard," *Aeronautical Journal*, Vol. 106, 2002, pp. 413–426.

[2]Rossow, V. J., "Lift-Generated Vortex Wakes of Subsonic Transport Aircraft," *Progress in Aerospace Sciences,* Vol. 35, 1999, pp. 507–660.

[3]Crouch, J. D., Miller, G. D., and Spalart, P. R., "Active-Control System for Breakup of Airplane Trailing Vortices," *AIAA Journal*, Vol. 39, 2001, pp. 2374–2381.

[4]Glauert, H., *The Elements of Aerofoil and Airscrew Theory*, 2nd ed., Cambridge Univ. Press, Cambridge, England, U.K., 1947, Chap. 11.

[5]Schmitz, F. W., *Aerodynamik des Flugmodells, Tragfluegelmessungen I*, 3rd ed., Carl Lange Verlag, Duisburg, Germany, 1957, pp. 89–94.

A. Plotkin
Associate Editor